

Somatostatin Receptor-Mediated Specific Delivery of Paclitaxel Prodrugs for Efficient Cancer Therapy

MEIRONG HUO, QINNV ZHU, QU WU, TINGJIE YIN, LEI WANG, LIFANG YIN, JIANPING ZHOU

State Key Laboratory of Natural Medicines, Department of Pharmaceutics, China Pharmaceutical University, Nanjing 210009, China

Received 9 January 2015; revised 1 March 2015; accepted 5 March 2015

Published online 27 March 2015 in Wiley Online Library (wileyonlinelibrary.com). DOI 10.1002/jps.24438

ABSTRACT: In this study, a novel PTX prodrug, octreotide(Phe)–polyethylene glycol–paclitaxel [OCT(Phe)–PEG–PTX], was successfully synthesized and used for targeted cancer therapy. A nontargeting conjugate, mPEG–PTX, was also synthesized and used as a control. Chemical structures of OCT(Phe)–PEG–PTX and mPEG–PTX were confirmed using ^1H nuclear magnetic resonance and circular dichroism. The drug contents in both the conjugates were 12.0% and 14.0%, respectively. Compared with the parent drug (PTX), OCT(Phe)–PEG–PTX, and mPEG–PTX prodrugs showed a 20,000- and 30,000-fold increase in water solubility, respectively. PTX release from mPEG–PTX and OCT(Phe)–PEG–PTX exhibited a pH-dependent profile. Moreover, compared with mPEG–PTX, OCT(Phe)–PEG–PTX exhibited significantly stronger cytotoxicity against NCI-H446 cells (SSTR overexpression) but comparable cytotoxicity against WI-38 cells (no SSTR expression). Results of confocal laser scanning microscopy revealed that the targeting prodrug labeled with fluorescence probe was selectively taken into tumor cells via SSTR-mediated endocytosis. *In vivo* investigation of prodrugs in nude mice bearing NCI-H446 cancer xenografts confirmed that OCT(Phe)–PEG–PTX prodrug exhibited stronger antitumor efficacy and lower systemic toxicity than mPEG–PTX and commercial Taxol. These results suggested that OCT(Phe)–PEG–PTX is a promising anticancer drug delivery system for targeted cancer therapy. © 2015 Wiley Periodicals, Inc. and the American Pharmacists Association *J Pharm Sci* 104:2018–2028, 2015

Keywords: prodrugs; cancer chemotherapy; targeted drug delivery; peptide delivery; polymeric drugs

INTRODUCTION

Paclitaxel (PTX) exhibited a significant activity against various solid tumors because of its ability to promote tubulin assembly into microtubules.¹ However, serious drawbacks hamper the clinical application of PTX. First, PTX lacks selective cytotoxicity against cancer cells and frequently leads to serious side effects.² Poor water solubility of PTX (0.3 $\mu\text{g}/\text{mL}$) is another concern that significantly reduces its wider clinical application. To enhance its water solubility, PTX is currently formulated as a 50:50 mixture of Cremophor EL and ethanol (Taxol). However, the amount of Cremophor EL required to solubilize PTX is considerably high (26 mL Cremophor EL for a single intravenous administration in an average patient), which leads to significant side effects such as hypersensitivity, neurotoxicity, nephrotoxicity, and cardiotoxicity.³

The prodrug strategy is promising to overcome these problems.^{4,5} Over the last decades, several studies have been conducted on prodrug synthesis of PTX. Poly(ethylene glycol) methyl ether methacrylate,⁶ cyclotriphosphazene,⁷ poly(vinyl alcohol),⁸ and poly(L-glutamic acid)⁹ have been proposed as PTX carriers. However, only a part of the prodrug can efficiently accumulate in the tumor site through the enhanced permeability and retention (EPR) effect, which decrease drug efficiency and increase its toxicity. Further improvement can be achieved by conjugating targeting ligands onto polymeric prodrugs to achieve selective delivery to tumor cells.¹⁰ Receptor-targeted polymeric prodrugs have been shown to improve therapeutic responses both *in vitro* and *in vivo*.¹¹

Various ligands have been investigated, including folate,¹² transferrin,¹³ antibodies,¹⁴ peptides,¹⁵ and aptamers.¹⁶

Somatostatin (SST) is a polypeptide that is released in the gastrointestinal tract by delta cells and the hypothalamus. It is a key regulatory peptide that inhibits hormones such as gastrin, cholecystokinin, glucagon, growth hormone, insulin, and secretin.¹⁷ Cellular actions of SST are mediated by five SST receptors (SSTR 1–5). SSTRs are G-protein-coupled receptors that are widely distributed in various tumors, including small cell lung cancer, neuroendocrine tumors, prostate cancer, breast cancer, colorectal carcinoma, gastric cancer, and hepatocellular carcinoma.^{18,19} Clinical usefulness of SST is limited by its very short half-life. Several synthetic SST analogs, including octreotide (OCT), lanreotide, and vapreotide, have improved metabolic stability and increased affinity to SSTRs.²⁰

Octreotide, one of the most extensively studied SST analogs, selectively binds to SSTR2 and SSTR5. It is composed of eight amino acids H₂N-D-Phe-Cys-Phe-D-Trp-Lys-Thr-Cys-Thr-ol (disulfide bridge Cys2-Cys7). OCT has been used clinically to prevent carcinoid crisis²¹ and to visualize tumors containing high density of SSTRs by using scintigraphy.²² For example, radiolabeled OCT derivatives, ^{99m}Tc-OCT and ¹¹¹In-OCT, are very useful for detecting small neuroendocrine tumors that cannot be detected by conventional methods.^{23,24} In addition to its successful application on radio-oncology, OCT is further used to enhance the delivery of drugs to tumor cells by modifying them on the surface of nanocarriers.^{25,26} These promising results prompted us to develop OCT as a specific targeting moiety for delivering a polymeric prodrug of PTX into tumor cells via SSTR endocytosis.

Polyethylene glycol (PEG) modification of drugs, also called PEGylation, is widely performed to improve the solubility and *in vivo* stability of drugs.²⁷ Use of PEG is widespread because of its unique physicochemical characteristics such as low

Correspondence to: Zhou Jianping (Telephone: +86-25-8327-1102; Fax: +86-25-8547-2579; E-mail: cpu.zhoujp@163.com)

Journal of Pharmaceutical Sciences, Vol. 104, 2018–2028 (2015)

© 2015 Wiley Periodicals, Inc. and the American Pharmacists Association

polydispersity in molecular weight and solubility in aqueous as well as many organic solvents.²⁸ Moreover, PEGylation prevents rapid renal clearance of drugs and decreases their uptake by mononuclear phagocyte system, thus prolonging their *in vivo* half-life.²⁹ In addition, passive tumor targeting of drugs can be achieved by their PEGylation through the EPR effect.³⁰

In this study, a novel polymeric prodrug system of OCT(Phe)-PEG-PTX was developed for targeted tumor therapy. Targeting ligand OCT helps in achieving high local concentrations of antitumor drugs to improve therapeutic efficiency, and water-soluble PEGs improve water solubility of parent drugs and improve the pharmacokinetic profile of PTX while reducing its side effects. Nontargeted prodrug mPEG-PTX was prepared as a control. The present study investigated the aqueous solubilities of OCT(Phe)-PEG-PTX and mPEG-PTX and *in vitro* release profiles of parent drugs from polymeric drugs. Then, the cytotoxicity, cellular uptake, and intracellular distribution of prodrugs were evaluated on human nonsmall lung cancer cells (NCI-H446; SSTR overexpression) and human embryonic lung fibroblasts (WI-38 cells, no SSTRs expression). Finally, *in vivo* antitumor efficacy and systemic toxicity of OCT(Phe)-PEG-PTX on nude mice bearing NCI-H446 cancer xenografts were compared with those of nontargeting mPEG-PTX and Taxol formulation.

MATERIALS AND METHODS

Materials

Paclitaxel was obtained from Chongqing Meilian Pharmaceutical Company, Ltd. (Chongqing, China). OCT (molecular weight, 1019.26 Da) was kindly provided by Shanghai Soho-Yiming Pharmaceuticals Company, Ltd. (Shanghai, China). Succinic anhydride (SA) was purchased from Shanghai LingFeng Reagent Company, Ltd. (Shanghai, China), and 1-ethyl-3-(3-dimethylaminopropyl) carbodiimide hydrochloric acid salt (EDC-HCl) was purchased from GL Biochem (Shanghai, China). Methoxypolyethylene glycol amine (mPEG-NH₂; molecular weight, 5000 Da) and *N*-hydroxysuccinimide (NHS) were purchased from Aladdin Reagent Company Ltd. (Shanghai, China). Succinimidyl carboxymethyl ester (SCM, Boc-NH-PEG-NHS) was obtained from Creative PEGWorks (Winston-Salem, North Carolina), and 3-(4,5-dimethylthiazol-2-yl)-2,5-diphenyltetrazolium bromide (MTT) was purchased from Sigma Chemical Company (St. Louis, Missouri). Cremophor EL was kindly gifted by BASF Corporation (Ludwigshafen, Germany). All other reagents were of analytical grade and were used without further purification. Distilled and deionized (DI) water was used in all experiments.

Methods

Synthesis of OCT(Phe)-PEG-PTX and mPEG-PTX Prodrugs

Octreotide(Phe)-PEG-PTX and mPEG-PTX were synthesized using a three-step procedure, according to the general scheme presented in Scheme 1.

Synthesis of 2'-O-Succinyl-Paclitaxel

2'-O-Succinyl-Paclitaxel (2'-SA-PTX) was synthesized as previously reported.³¹ The crude product was purified by silica gel column chromatography with ethyl acetate-*n*-hexane-ethyl

acid (6:1:0.1) as eluent to give the intermediate (yield = 90.8%) for the next step.

Synthesis of OCT(Phe)-PEG-NH₂

Octreotide was conjugated to Boc-NH-PEG-NHS using the following procedure. Briefly, Boc-NH-PEG-NHS, OCT, and EDC-HCl were dissolved in 5 mL acetonitrile (molar ratio of Boc-NH-PEG-NHS:OCT = 3:1) in the presence of 5 μ L triethylamine. The mixture was stirred at 4°C for 12 h. Because OCT could be PEGylated at the N-terminus (phenylalanine, Phe) and the lysine (Lys) residue, the crude product was purified by loading directly onto a reversed-phase high-performance liquid chromatography (HPLC) system (LC-10AT; Shimadzu, Kyoto, Japan) with Delta-Pak C₁₈ 25 \times 100 mm² column and eluted with an acetonitrile gradient (35%–50%, v/v) in water [0.1% trifluoroacetic acid (TFA)] at a column temperature of 25°C. The flow rate was 1.0 mL/min, and UV absorbance was monitored at 280 nm. Then, the separated OCT(Phe)-PEG-NH-Boc was deprotected to obtain OCT(Phe)-PEG-NH₂ in the solvent of acetonitrile-TFA (80/20) solutions using an ice-water bath under argon.

Synthesis of OCT(Phe)-PEG-PTX and mPEG-PTX

Octreotide(Phe)-PEG-PTX and mPEG-PTX were synthesized by coupling the carboxyl group of 2'-SA-PTX with the amine group of OCT(Phe)-PEG-NH₂ and mPEG-NH₂, respectively, in the presence of EDC-HCl and NHS. Briefly, 24 mg 2'-SA-PTX was dissolved in 4 mL DMF. EDC-HCl (20 mg) and NHS (20 mg) were successively added to the above solutions. The mixture was stirred at room temperature for 2 h. Then, 120 mg OCT(Phe)-PEG-NH₂ or 100 mg mPEG-NH₂ dissolved in 2 mL DMF was added, and the mixture was stirred for another 24 h. Progress of the reaction was monitored by TLC [ethyl acetate:*n*-hexane = 6:1 (v/v)]. After the reaction was complete, DI water was added gradually, and the solution was dialyzed against DI water for 48 h (MWCO, 3.5 kDa) followed by lyophilization. The yield of OCT(Phe)-PEG-PTX and mPEG-PTX was 89.3% and 92.4% with respect to the PTX, respectively. The high yields could potentially assist in the industrialization of the conjugate manufacturing process. The resulting products were stored at 4°C until further use.

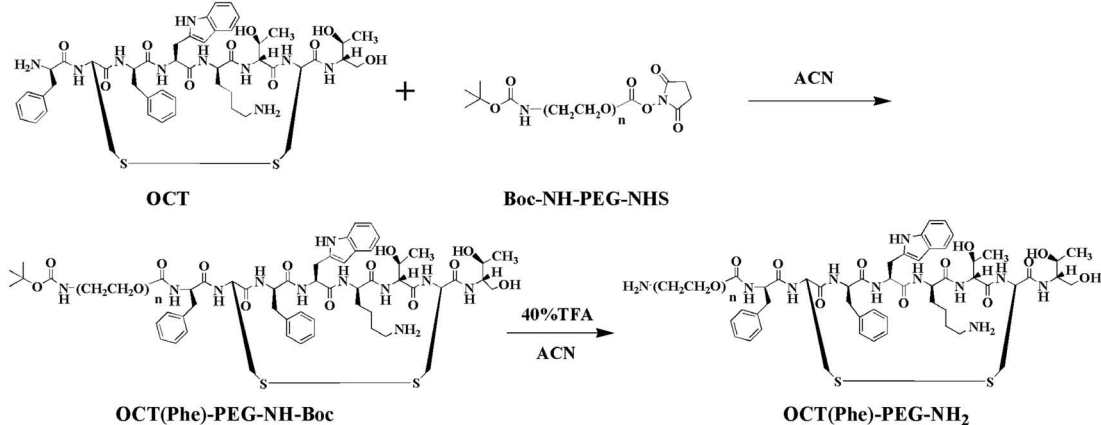
Characterization of 2'-SA-PTX, OCT(Phe)-PEG-NH₂, OCT(Phe)-PEG-PTX, and mPEG-PTX

Chemical structures of 2'-SA-PTX, OCT(Phe)-PEG-NH₂, OCT(Phe)-PEG-PTX, and mPEG-PTX were confirmed using a 500-MHz Avance Bruker NMR spectrometer, with OCT, mPEG, and PTX as controls. PTX, 2'-SA-PTX, OCT(Phe)-PEG-PTX, and mPEG-PTX were dissolved in CDCl₃, and OCT, mPEG, and OCT(Phe)-PEG-NH₂ were dissolved in D₂O.

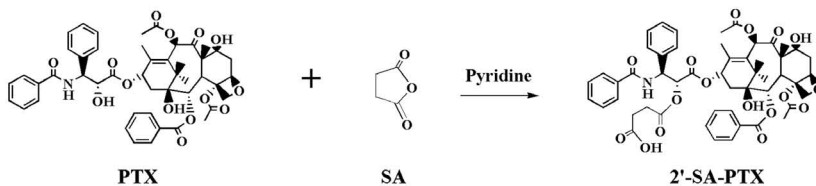
Circular dichroism (CD) spectra of OCT, OCT(Phe)-PEG-NH₂, and OCT(Phe)-PEG-PTX were recorded in the range of 190–250 nm by using Jasco J-810 spectropolarimeter (Jasco, Easton, Maryland) with a CD cell of 0.1-cm path length and 1-nm bandwidth. Scan speed of 100 nm/min was used, and in all six scans were performed per sample. The spectra were expressed as mean residue molar ellipticity in deg·cm²/dmol. Peptide concentrations were set at 100 μ g/mL in 0.01 M phosphate buffer (pH 7.4).

Drug concentration in OCT(Phe)-PEG-PTX and mPEG-PTX prodrugs was determined using ultraviolet visible

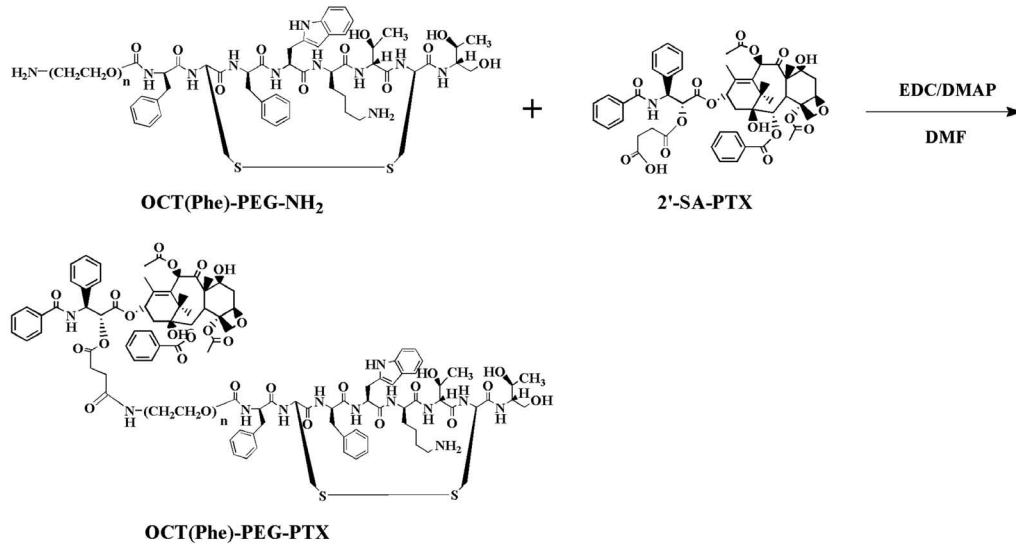
Step 1: Synthesis of OCT-PEG-NH₂



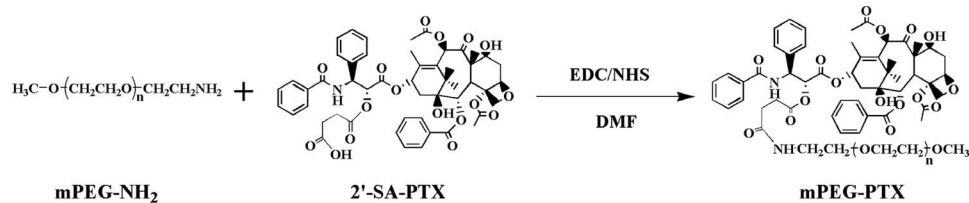
Step 2: Synthesis of 2'-SA-PTX



Step 3(a): Synthesis of OCT(Phe)-PEG-PTX



Step 3(b): Synthesis of mPEG-PTX



Scheme 1. Scheme for synthesizing OCT(Phe)-PEG-PTX and mPEG-PTX prodrugs.

spectrophotometer analysis (UV-Vis; TU-1800; Beijing Purkinje General Instrument Company Limited, Beijing, China) based on a standard curve generated with known concentrations of PTX in methanol ($\lambda = 227$ nm) and by assuming that the PTX prodrug and free drug had the same molar extinction coefficients in water and in methanol, respectively, and that both followed the Beer–Lambert law.³²

Solubilities of OCT(Phe)–PEG–PTX and mPEG–PTX prodrugs were evaluated using a visual observation method.⁸

In Vitro Release of PTX from OCT(Phe)–PEG–PTX and mPEG–PTX Prodrugs

In vitro release of PTX from OCT(Phe)–PEG–PTX and mPEG–PTX were evaluated using a dialysis method. Lyophilized prodrugs containing 0.5 mg PTX were dissolved in 1 mL phosphate buffered saline (PBS) (0.1 M, pH 7.4 and 5.8, respectively). The resulting solutions were placed inside a dialysis bag (MWCO, 3.5 kDa), and the entire bag was sunk in 150 mL PBS (0.1 M, pH 7.4 and 5.8, respectively) at 37°C supplemented with 0.1% (w/v) Tween 80. An aliquot (2 mL) was drawn at predetermined time intervals, and fresh release medium (2 mL, 37°C) was added. The concentration of free PTX in the samples was determined using HPLC (LC-2010 system; Shimadzu) equipped with a LICHrospher™ C18 column (particle size, 5 μ m; 250 \times 4.6 mm²). The mobile phase consisted of acetonitrile/35 mM ammonium acetate [55:45 (v/v), pH 5.5] and had a flow rate of 1.0 mL/min. The detection wavelength was 227 nm, and sample injection volume was 20 μ L.

In Vitro Cell Studies

Cell Culture

NCI-H446 cells (SSTR overexpression) and WI-38 cells (no SSTR expression) were obtained from Origin Biosciences Inc. (Nanjing, China) and cultured in RPMI 1640 medium supplemented with 10% fetal bovine serum and 0.1% penicillin/streptomycin at 37°C in 5% CO₂ atmosphere. All culture media were replaced every 3 days. Cells in their growth phase were used for performing the experiments.

Cytotoxicity Assay

In vitro cytotoxicity of OCT(Phe)–PEG–PTX and mPEG–PTX prodrugs was evaluated with NCI-H446 and WI-38 cells by using the MTT assay. Both the cells were seeded in 96-well plates at a density of 5 \times 10³ cells/well and were incubated for 24 h at 37°C. Next, the cells were incubated with 100 μ L OCT(Phe)–PEG–PTX, mPEG–PTX, and Taxol (at equivalent PTX concentration of 0.02, 0.08, 0.16, 0.32, 0.64, and 1.28 μ g/mL) diluted in OCT-deficient RPMI 1640 medium at 37°C for 72 h. Taxol, which is a commercial formulation, was prepared by dissolving 12 mg PTX in 1.0 mL ethanol and 1.0 mL of Cremophor EL, followed by sonication for 30 min.³³ Then, the MTT assay was conducted according to previously reported procedures.³⁴ Toxicity of PTX formulations was expressed as inhibitory concentration at which 50% of cell growth is inhibited (IC₅₀).

Intracellular Uptake and Distribution of Fluorescence-Labeled Prodrugs. To evaluate the intracellular uptake and distribution of PTX-polymeric prodrugs in NCI-H446 cell lines, a fluorescence probe 6-tetramethylrhodamine isothiocyanate (TRITC) was chemically coupled with mPEG–NH₂ and

OCT(Phe)–PEG–NH₂ based on the protocol for preparing PTX-polymeric prodrugs. CLSM was employed to examine the intracellular uptake and distribution of OCT(Phe)–PEG–TRITC and mPEG–NH₂–TRITC. NCI-H446 cells were seeded in 6-well plates and were incubated for 24 h. Next, 2 μ M each of OCT(Phe)–PEG–TRITC and mPEG–NH₂–TRITC were added to respective wells, and the cells were incubated for another 4 h at 37°C. The nuclei of the cells were stained using a blue molecular probe Hoechst 33342 for 10 min. The cells were washed six times with growth medium. Intracellular distribution of fluorescence probe was examined using Zeiss LSM 510 META confocal laser scanning microscope (Carl Zeiss, Jena, Germany) at excitation and emission wavelengths of 455 and 572 nm, respectively. The nuclei were imaged at excitation and emission wavelengths of 352 and 544 nm, respectively.

In the receptor-competitive inhibition experiment, 2 mM OCT was added to the medium and incubated for 1 h. The cells were incubated for another 4 h with OCT(Phe)–PEG–TRITC to evaluate the active targeting of OCT. Nuclear staining and determination of intracellular TRITC distribution were performed as described above.

In Vivo Antitumor Efficacy Test. BALB/c nude mice (age, 7 weeks; weight, 20–25 g) were used for pharmacodynamic experiments. A subcutaneous tumor was established by inoculating 5 \times 10⁶ NCI-H446 cells into the armpit region of these mice. When the tumors grew to approximately 100 mm³, the mice were randomly divided into four groups to receive different injections as follows: (1) normal saline (control group, $n = 5$); (2) Taxol at 10 mg PTX/kg ($n = 5$); (3) OCT(Phe)–PEG–PTX at 10 mg PTX/kg ($n = 5$); and (4) mPEG–PTX at 10 mg PTX/kg ($n = 5$). Each sample was injected once every 5 days for 15 days. Body weights of mice were recorded, and tumor volumes were calculated using the following equation: $a \times b^2/2$, where a was the largest diameter and b was the smallest diameter. Tumors were also removed from the sacrificed mice after 20 days of observation and were weighed. Percentage of tumor weight inhibition (%TWI) was calculated using the following formula: $\text{TWI} (\%) = (W_C - W_D)/W_C \times 100$, where W_C and W_D were the mean tumor weights of control and treated groups, respectively.

To further evaluate the antitumor effect of Taxol and PTX-polymeric prodrugs on the tumor bearing animals, the tumors were fixed in 10% formalin. Formalin-fixed tumors were embedded in paraffin blocks to prepare hematoxylin and eosin (H&E)-stained tumor sections. These sections were visualized under an optical microscope (Olympus, Tokyo, Japan).

Blood samples were collected after 20 day of observation. Biological markers of liver and kidney function, that is, alanine transaminase (ALT), aspartate transaminase (AST), alkaline phosphatase (ALP), blood urea nitrogen (BUN), and serum creatinine (SCr), were measured using blood samples.

Statistical Analysis

Statistical analysis was performed using Student's *t*-test for two groups and one-way analysis of variance for multiple groups. All the results are expressed as mean \pm SD, unless otherwise noted. The *p* values less than 0.05 were considered statistically significant.

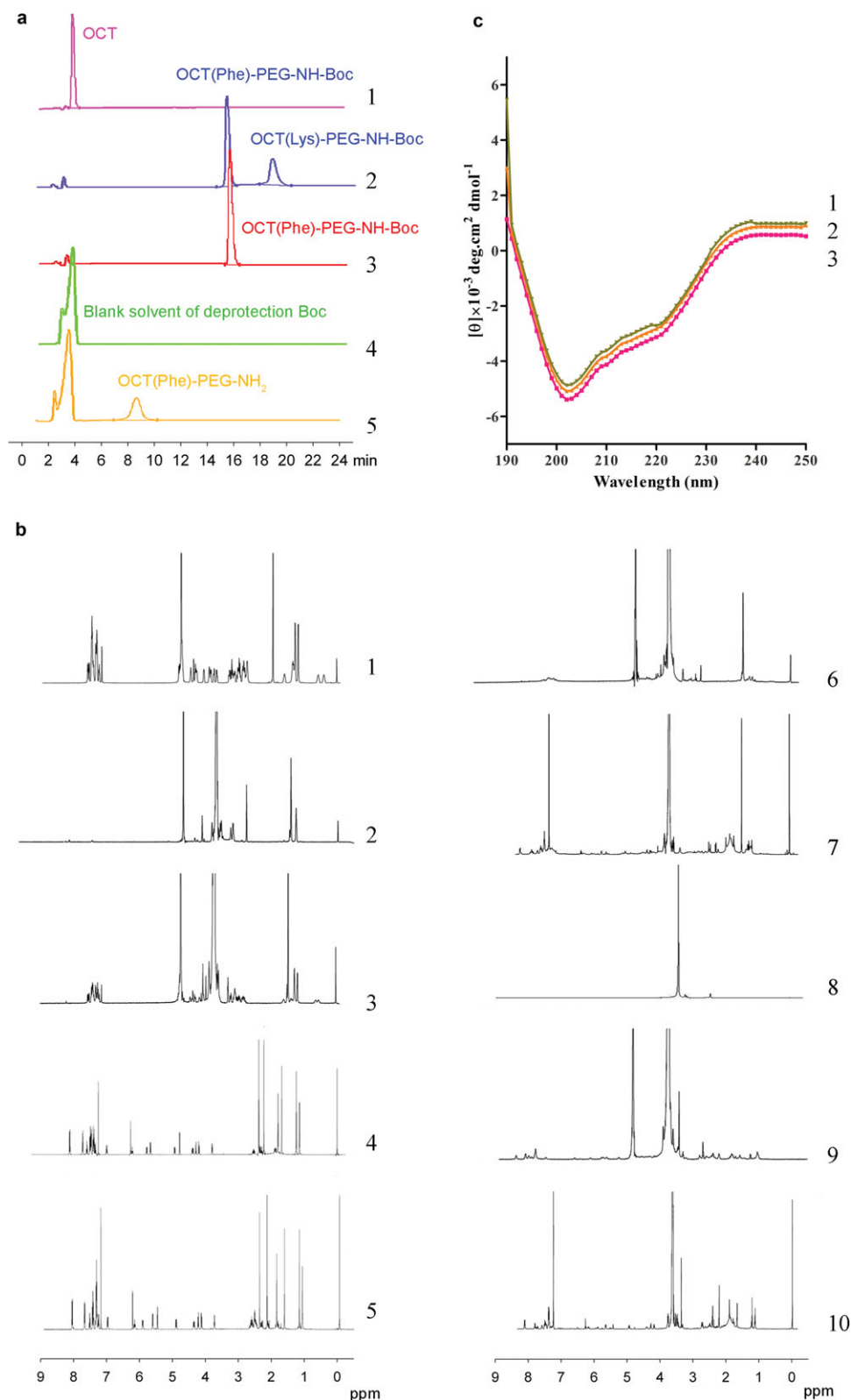


Figure 1. (a) HPLC analysis of OCT (1) before separation (2) and after separation (3) of the reaction mixture and blank solvent of deprotected Boc (4) and OCT(Phe)-PEG-NH₂ (5). (b) The ¹H-NMR spectra of OCT in D₂O (1), Boc-NH-PEG-NHS in D₂O (2), OCT(Phe)-PEG-NH₂ in D₂O (3), PTX in CDCl₃ (4), 2'-SA-PTX in CDCl₃ (5), OCT(Phe)-PEG-PTX in D₂O (6), and CDCl₃ (7), mPEG-NH₂ in D₂O (8), and mPEG-PTX in D₂O (9), and CDCl₃ (10). (c) CD spectra of OCT. HAC (1), OCT(Phe)-PEG-NH₂ (2), and OCT(Phe)-PEG-PTX (3).

RESULTS AND DISCUSSION

Synthesis and Characterization of OCT(Phe)-PEG-PTX and mPEG-PTX Prodrugs

In an attempt to prepare the targeting polymeric prodrug OCT(Phe)-PEG-PTX, the ligand OCT was first conjugated to the carboxyl group of PEG by EDC reaction. The PEGylated reaction was preferred at two sites containing a primary amine: the N-terminus (Phe) and the lysine (Lys) residue. Several studies have shown that N-terminus modifications of OCT effectively retain the binding affinity to SSSTR-overexpressing tumor cells.^{35,36} Therefore, it was necessary to separate the by-products. As shown in Figure 1a, the developed HPLC method could separate OCT(Lys)-PEG-NH-Boc from unmodified OCT and OCT(Phe)-PEG-NH-Boc. Because of ionic polarity difference, the OCT was washed out, followed by OCT(Phe)-PEG-NH-Boc and OCT(Lys)-PEG-NH-Boc (Fig. 1a2). The HPLC chromatogram of OCT(Phe)-PEG-NH-Boc product is shown in Figure 1a3. After deprotection of Boc, the polarity of OCT(Phe)-PEG-NH₂ increased, resulting in the forward movement of the chromatographic peak (Fig. 1a5). Next, 2'-SA-PTX was prepared by esterification of 2'-hydroxyl group by using SA in the presence of dry pyridine. After 3 h of reaction, no free PTX was found by TLC, indicating that the reaction was complete. The product was collected as a white powder, with a yield of 89% and purity of 98%, respectively. Finally, by using EDC and NHS as reaction promoters, 2'-SA-PTX was conjugated to the free amines of OCT(Phe)-PEG-NH₂ through amide bond linkage to produce OCT(Phe)-PEG-PTX.

Chemical structures of the synthesized 2'-SA-PTX, OCT(Phe)-PEG-NH₂, and OCT(Phe)-PEG-PTX were confirmed using ¹H-NMR. The ¹H-NMR spectra of 2'-SA-PTX are shown in Figure 1b5. Compared with the spectra of PTX (Fig. 1b4), the characteristic peaks of SA appeared at 2.5–2.8 ppm (-O-CO-CH₂-CH₂-), and the chemical shift of 2'-hydroxyl group of PTX changed from 4.8 to 6.0 ppm because of succinylation. The ¹H-NMR analysis confirmed the successful introduction of SA into PTX. Succinylation took place preferentially at the 2'-hydroxyl group position of PTX. The ¹H-NMR spectra of OCT(Phe)-PEG-NH₂ are shown in Figure 1b3. Compared with the spectra of OCT (Fig. 1b1) and Boc-NH-PEG-NHS (Fig. 1b2), the peaks at 7.0–7.5 ppm and 3.52–3.64 ppm belonged to the typical protons of OCT and PEG, respectively, indicating that PEG was successfully coupled with the N-terminal amine of OCT. Furthermore, successful conjugation of 2'-SA-PTX to the amine group of OCT(Phe)-PEG-NH₂ was confirmed by the characteristic peaks of 2'-SA-PTX at 2.5–2.8 ppm (SA) and 7.1–7.6 ppm (benzene ring), with some overlap with OCT in the ¹H-NMR spectra of OCT(Phe)-PEG-PTX (Figs. 1b3 and 1b5–1b7).

Structural conformation of OCT in OCT(Phe)-PEG-NH₂ and OCT(Phe)-PEG-PTX was further evaluated using CD, with OCT as the control. As shown in Figure 1c, the CD spectra of intact OCT, OCT(Phe)-PEG-NH₂, and OCT(Phe)-PEG-PTX were nearly superimposable in the range of 190–250 nm, suggesting that PEGylation and conjugation of 2'-SA-PTX had no significant effect on the secondary structure of OCT.³⁷

As a nontargeting control, mPEG-PTX was also synthesized by conjugating 2'-SA-PTX with mPEG-NH₂. The chemical structure of mPEG-PTX was also confirmed using ¹H-NMR. Compared with the spectra of mPEG-NH₂ (Fig. 1b8) and 2'-

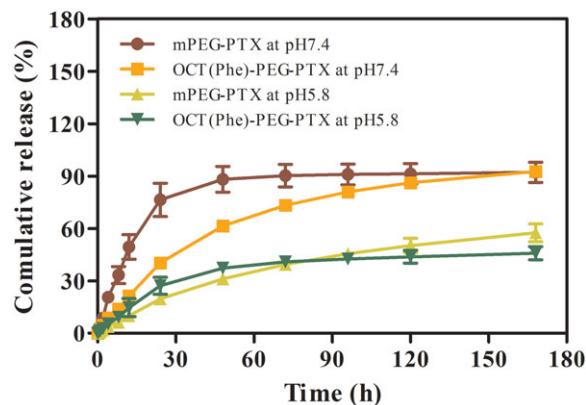


Figure 2. *In vitro* PTX release profiles of (a) mPEG-PTX and OCT(Phe)-PEG-PTX in neutral (pH 7.4) and acidic conditions (pH 5.8) at 37°C. Each point is represented in mean \pm SD ($n = 6$).

SA-PTX (Fig. 1b5), the peaks at 2.5–2.8 and 7.5–8.0 ppm belonged to the typical protons of mPEG and benzene ring of 2'-SA-PTX, respectively, in ¹H-NMR spectra of mPEG-2'-SA-PTX (Figs. 1b9 and 1b10). The results indicated that mPEG was successfully conjugated to 2'-SA-PTX.

Drug Concentration and Solubility of PTX in OCT(Phe)-PEG-PTX and mPEG-PTX

Concentrations of PTX in the polymeric prodrugs were quantified using UV absorbance ($\lambda = 227$ nm) by assuming that the prodrugs and free drug had the same molar extinction coefficients in water and methanol, respectively, and that both followed the Beer-Lambert law. The calculated weight of PTX in OCT(Phe)-PEG-PTX and mPEG-PTX was 12.0% (w/w) and 14.0% (w/w), respectively, which was consistent with the theoretical weight of PTX in OCT(Phe)-PEG-PTX [12.2% (w/w)] and mPEG-PTX (14.3%).

Solubility of PTX in PTX-polymeric prodrugs was determined using a direct observation method.⁸ The solubility of OCT(Phe)-PEG-PTX and mPEG-PTX prodrugs was 5.96 mg/mL (PTX equivalent) and 9.38 mg/mL (PTX equivalent), respectively, which was 20,000- and 30,000-fold higher than that of the parent drug (PTX, 0.3 μ g/mL). The results showed that PEG modification could significantly improve the solubility of PTX.

In Vitro Release of PTX from OCT(Phe)-PEG-PTX and mPEG-PTX

To investigate the stability of ester bond, we measured free PTX released from the two prodrugs after incubating the products in PBS at pH 7.4 and 5.8, respectively, at 37°C. Free PTX was measured using HPLC, as described above. The cumulative release rate curves are depicted in Figure 2. All the prodrugs exhibited a slow release profile, and the amount of PTX released from the prodrugs increased as the pH of the PBS increased. After 168 h of incubation in PBS at pH 7.4, PTX released from OCT(Phe)-PEG-PTX and mPEG-PTX prodrugs was approximately 92.63% and 92.03%, respectively. However, only approximately 45.84% and 57.54% of PTX was released from OCT(Phe)-PEG-PTX and mPEG-PTX prodrugs, respectively, after 168 h of incubation in PBS at pH 5.8. However, there are many contradictory results reported in literature. Some studies showed quicker free drug release from prodrugs

at pH 5.5 than pH 7.4,³⁸ whereas competing studies observed a contrary phenomena.³¹ These prodrugs were all synthesized by conjugating different macromolecules to the 2' position of PTX through a spacer succinyl group. Cavallaro et al.³¹ also pointed out that the free PTX degraded both at pH 5.5 and 7.4 by chemical pathways. Therefore, the PTX release and degradation took place simultaneously. They also studied the *in vitro* release of free PTX for 2'-SA-PTX and poly(hydroxyethylaspartamide)-2'-SA-PTX (PHEA-2'-SA-PTX) conjugates at pH 5.5 and 7.4, respectively. A different release profile was observed. In the case of 2'-SA-PTX, more released PTX was determined at pH 5.5 than pH 7.4. However, in the case of PHEA-2'-SA-PTX, more free PTX was determined at pH 7.4 than 5.5. Therefore, both the pH and the stability of free PTX and its derivatives at different pH environments can affect the free PTX we determined in the release media.

In Vitro Cytotoxicity Studies

To evaluate the selectivity of OCT(Phe)-PEG-PTX, cytotoxicities of mPEG-PTX and OCT(Phe)-PEG-PTX against NCI-H446 (SSTR overexpression) and WI-38 cells (no SSTR expression) were compared. Figure 3 shows the IC₅₀ values of Taxol, mPEG-PTX, and OCT(Phe)-PEG-PTX prodrugs against NCI-H446 and WI-38 cells. After 72 h of incubation, mPEG-PTX had significantly higher IC₅₀ values against NCI-H446 cells than Taxol ($p < 0.05$; Fig. 3a). This may be because free PTX is readily diffused into the cytosol by passive diffusion. In contrast, a common polymeric prodrug such as mPEG-PTX has to be internalized by endocytosis, after which the chemically conjugated drug is progressively released via ester bond hydrolysis by both chemical and enzymatic pathways; this usually delays the cytosolic delivery of the drug and decreases the efficacy of cancer cell inhibition.³⁹ However, when the polymeric prodrug was modified with OCT, the IC₅₀ values significantly decreased. The IC₅₀ value of OCT(Phe)-PEG-PTX prodrug was 2.6-fold lower than that of the mPEG-PTX prodrug. The enhanced cytotoxicity of OCT(Phe)-PEG-PTX might be attributed to its selective binding to the SSTRs expressed on the surface of NCI-H446 cells.

To further prove that the enhanced cellular uptake was because of receptor-mediated endocytosis of the polymeric prodrug, SSTR-deficient WI-38 cells were used for the cytotoxicity experiment. Figure 3b shows that the enhanced cytotoxicity of OCT(Phe)-PEG-PTX prodrug was observed only against NCI-H446 cells and not against WI-38 cells. On the basis of these cytotoxicity results, it can be concluded that OCT-modified polymeric prodrugs could increase the selectivity for killing tumor cells.

Intracellular Uptake and Distribution of Polymeric Prodrugs Labeled with Fluorescence Probe

Intracellular uptake and distribution of the polymeric prodrug labeled with TRITC in NCI-H446 cells were comparatively estimated using CLSM (Fig. 4). In the absence of OCT in the incubation medium, the intracellular fluorescence intensity of the OCT(Phe)-PEG-TRITC increased significantly (Fig. 4b) compared with that of the mPEG-TRITC (Fig. 4a). This result indicated that receptor-mediated endocytosis was involved in the cellular uptake of OCT-modified polymeric drug. PTX is a microtubule stabilizer, and enhanced localization of PTX in the

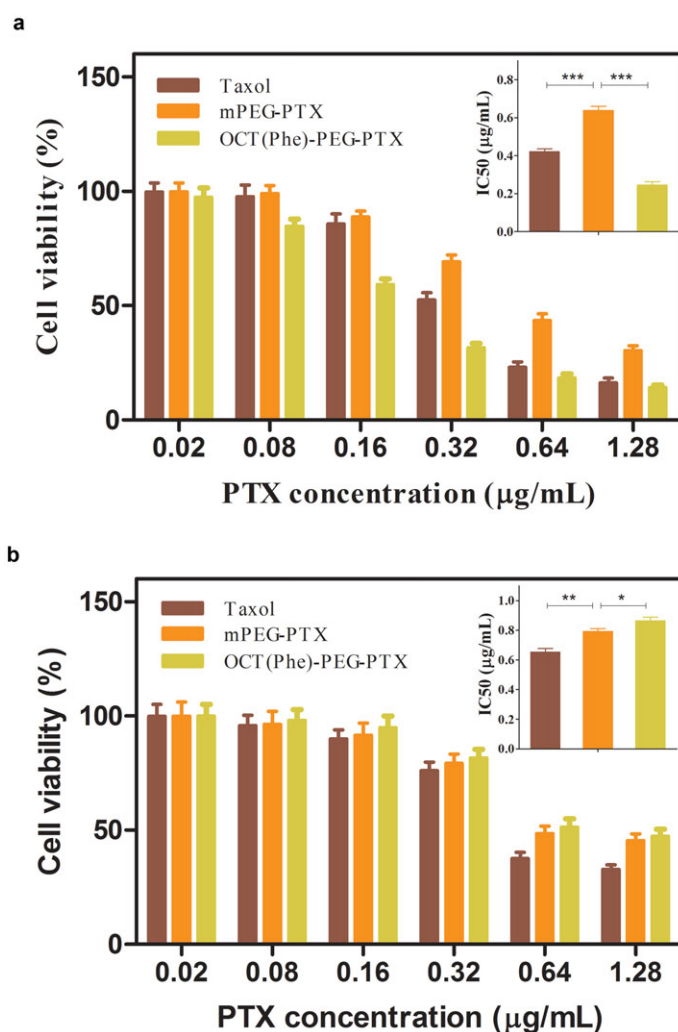


Figure 3. Cytotoxicities of Taxol, mPEG-PTX, and OCT(Phe)-PEG-PTX against NCI-H446 (a) and WI-38 cells (b) and their IC₅₀ values. Data are shown as mean \pm SD ($n = 3$). * $p < 0.05$, ** $p < 0.01$, and *** $p < 0.001$.

cytoplasm facilitates the elicitation of its pharmacological responses. These results were in line with those obtained in the cytotoxicity assay. Interestingly, fluorescence intensities of the nuclei of cells incubated with the OCT(Phe)-PEG-TRITC were much greater than those of nuclei of cells incubated with the mPEG-TRITC. This might be because SSTR-mediated endocytosis could transport higher proportions of the active polymeric prodrug within the cytoplasm, thus increasing the probability of fluorescence probes to enter the nucleus. This result suggested that a novel polymeric prodrug might be obtained by conjugating DNA-toxin to OCT(Phe)-PEG-NH₂.

Competition experiment showed that in the presence of the blocking ligand, fluorescence intensity of OCT-PEG-TRITC reduced dramatically and became equivalent to that of the mPEG-TRITC (Fig. 4c). Overall, the results of CLSM directly indicated that OCT-modified polymeric prodrug was taken up by SSTR-mediated endocytosis, which was consistent with the results of flow cytometry.

It should be noted that as PTX molecules possess no fluorescent characteristics, the hydrophobic fluorescence

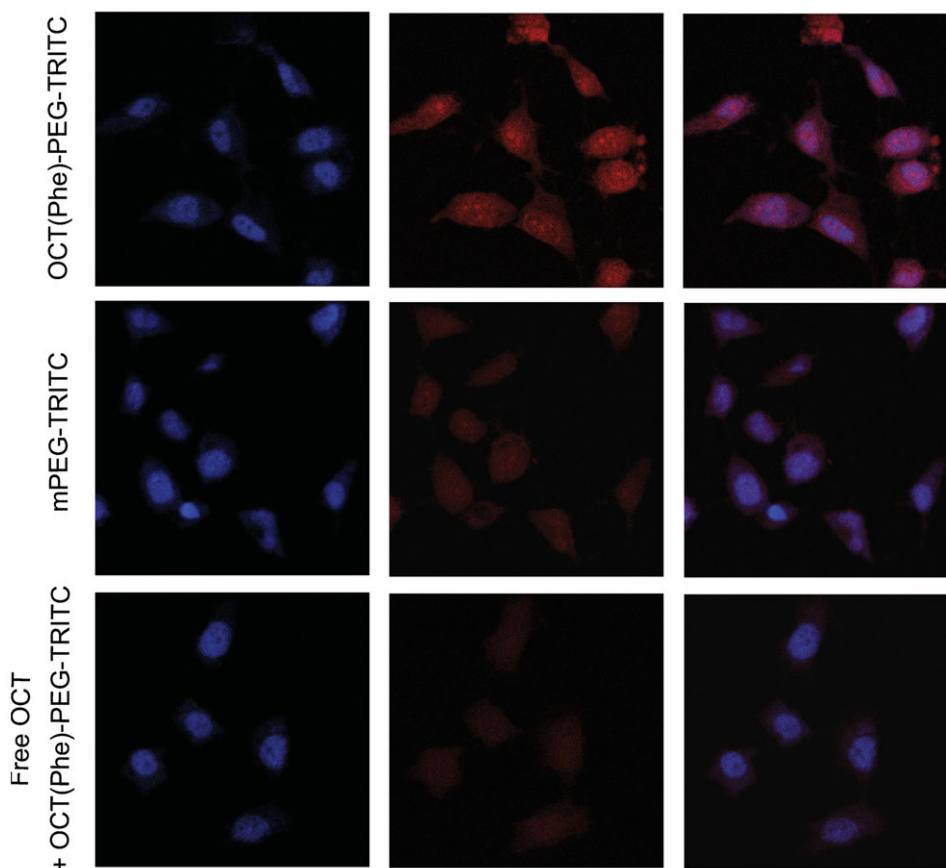


Figure 4. Confocal microscopy images of NCI-H446 cells after 4 h of *in vitro* exposure to mPEG-TRITC (a) and OCT(Phe)-PEG-TRITC (b) in the absence of free OCT in the medium and OCT(Phe)-PEG-TRITC in the presence of free OCT in the medium (c) at 37°C. For each panel, images from left to right show cell nuclei stained with Hoechst 33342 (blue), TRITC fluorescence in cells (red), and overlay of the two images.

probe TRITC was chosen as an alternative of PTX to for visualization under CLSM. However, TRITC does not possess similar pharmacological activities as PTX, such as microtubule targeting. Moreover, the physicochemical properties of TRITC and PTX are not identical. Therefore, the observed cellular uptake and distribution of OCT(Phe)-PEG-TRITC or mPEG-TRITC cannot entirely reflect the profiles of OCT(Phe)-PEG-PTX or mPEG-PTX. In future studies, a more reasonable method for detecting intracellular behavior of prodrugs will be of benefit.

***In Vivo* Antitumor Activity and Toxicity**

***In Vivo* Antitumor Activity**

In vivo antitumor efficacies of Taxol, mPEG-PTX, and OCT(Phe)-PEG-PTX were evaluated in NCI-H446 xenograft models. All PTX formulations were effective in preventing tumor growth compared with saline (Fig. 5). On the basis of the tumor volume (Fig. 5a), mPEG-PTX showed a comparable tumor growth suppression than Taxol. Moreover, OCT(Phe)-PEG-PTX exhibited the highest tumor growth inhibition efficacy among all PTX formulations. TIR values of OCT(Phe)-PEG-PTX, mPEG-PTX, and Taxol were calculated based on the tumor weight at the end of experiment (Fig. 5b). The TIR value of OCT(Phe)-PEG-PTX was 66.3%, which was 1.54- and

1.22-fold higher than that of mPEG-PTX and Taxol. Inhibition ratios calculated using tumor weight were consistent with the results of tumor volume measurements. The remarkable effect of OCT(Phe)-PEG-PTX on the suppression of tumor growth was also well supported by the histological analysis of the tumor cross-sections. Microscopic analysis of the H&E-stained section of the tumor tissue from the saline control group showed typical pathological characteristics of the tumor, such as closely arranged tumor cells (Fig. 5c). In contrast, the groups injected with Taxol, OCT(Phe)-PEG-PTX, and mPEG-PTX showed spotty necrosis and intercellular blank. Among the three therapeutic groups, tumor tissues from animals treated with OCT(Phe)-PEG-PTX showed the least number of tumor cells and the highest antitumor efficacy. The best therapeutic effect of OCT-modified PTX polymeric prodrug could be explained by the following aspects. First, PEGylation prevents the rapid renal clearance of drugs and their receptor-mediated uptake by the reticuloendothelial system, thus prolonging their *in vivo* half-life. Second, long-circulating polymers passively accumulate in the tumor tissue by the well-known EPR effect.⁴⁰ Third, modification of OCT results in fast cellular internalization through receptor-mediated endocytosis, as confirmed in cellular uptake studies, which further facilitates tumor targeting of polymeric prodrugs. Thus, OCT(Phe)-PEG-PTX has a promising potential to be used as a targeting carrier for efficient cancer therapy.

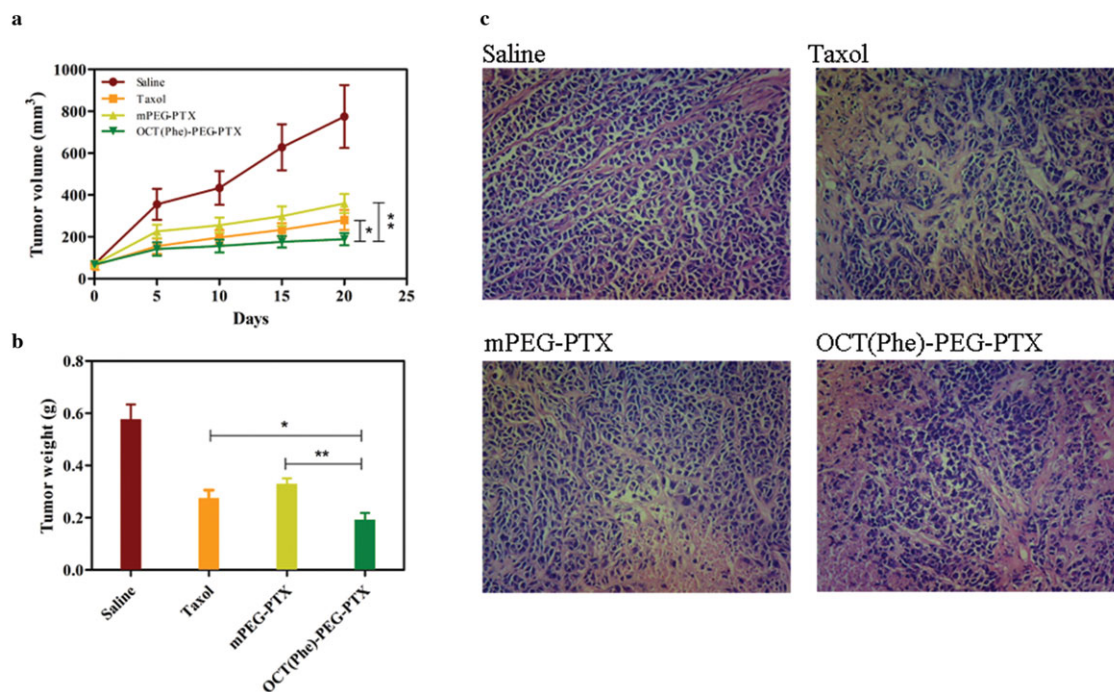


Figure 5. (a) Tumor growth inhibition in nude mice-bearing NCI-H446 cells after multiple injections of different PTX formulations. Data are expressed as mean \pm SD ($n = 5$). (b) Tumor weight in NCI-H446-bearing nude mice treated with saline, Taxol, mPEG-PTX, and OCT(Phe)-PEG-PTX ($n = 5$). (c) H&E staining shows growth inhibition of NCI-H446 cells in tumor tissue after treatment.

Evaluation of In Vivo Toxicity

Body weight is a crucial criterion to evaluate the systemic toxicity of PTX formulations. Figure 6a shows the variations in the relative body weights of mice with time. Compared with the initial body weights of tumor-bearing mice, no significant weight loss was observed after the administration of PTX-polymeric prodrugs, indicating that PTX-polymeric prodrugs were well tolerated at the tested dose. However, mice treated with the same dose of commercial Taxol showed significant weight loss during the first 10 days, after which the weight loss recovered slowly.

To evaluate the changes in hepatic and renal functions after PTX treatment, tumor-bearing mice were euthanized on day 20. Biochemical parameters such as ALT, AST, ALP, BUN, and SCr levels were determined (Figs. 6b and 6c). These levels were significantly elevated in the group treated with Taxol compared with those in the group receiving saline ($p < 0.001$). However, treatment with PTX-polymeric prodrug induced negligible changes in all the parameters, suggesting that PTX-polymeric prodrugs had lower hepatic and renal toxicity than Taxol.

CONCLUSIONS

In this study, OCT(Phe)-PEG-PTX was developed for targeted cancer therapy. The nontargeting prodrug mPEG-PTX was also synthesized and used as control. Drug content in OCT(Phe)-PEG-PTX and mPEG-PTX was 12.0% and 14.0%, respectively, and the aqueous solubility was 20,000- and 30,000-fold higher than that of the parent drug, respectively. *In vitro* release profiles showed that the release of PTX from mPEG-PTX and OCT(Phe)-PEG-PTX was much faster at pH 7.4 than at pH 5.8. Moreover, the targeting prodrug labeled with the fluores-

cence probe was selectively taken into tumor cells by SSTR-mediated endocytosis and exhibited significantly stronger cytotoxicity against NCI-H446 cells (SSTR overexpression) but comparable cytotoxicity against WI-38 cells (no SSTR expression) compared with the nontargeting control. In addition, *in vivo* investigation of micelles in nude mice-bearing NCI-H446 cancer xenografts confirmed that OCT(Phe)-PEG-PTX exhibited stronger antitumor efficacy and lower systemic toxicity than mPEG-PTX and commercial Taxol. Thus, the results of the present study indicated that OCT(Phe)-PEG-PTX had a great potential for use in targeted cancer therapy. Yet, significant refinement in terms of safety and activity in a more clinically accurate tumor model is required before the product can be applied to patients. This is the focus of our future work.

ACKNOWLEDGMENTS

This work was supported by the project of the National Natural Science Foundation of China (no. 81102397), the Natural Science Foundation of Jiangsu Province (no. BK2012761), Qing Lan Project of Jiangsu Province (no. 02432009), Fostering Plan of University Scientific and Technological Innovation Team of Jiangsu Qing Lan Project (2014). Innovative Project for Graduate Cultivation of Jiangsu Province (no. CXZZ11-0807), the Project Program of State Key Laboratory of Natural Medicines, China Pharmaceutical University (no. JKGQ201107 and JKPZ2013004), Key New Drug Innovation Project from the Ministry of Science and Technology of China (no. 2009ZX09310004) and National Basic Research Program of China (973 Program, no. 2009CB903300). The authors also acknowledge Michael Lin in the University of North Carolina at Chapel Hill for his kind editorial help in revising the English of this article.

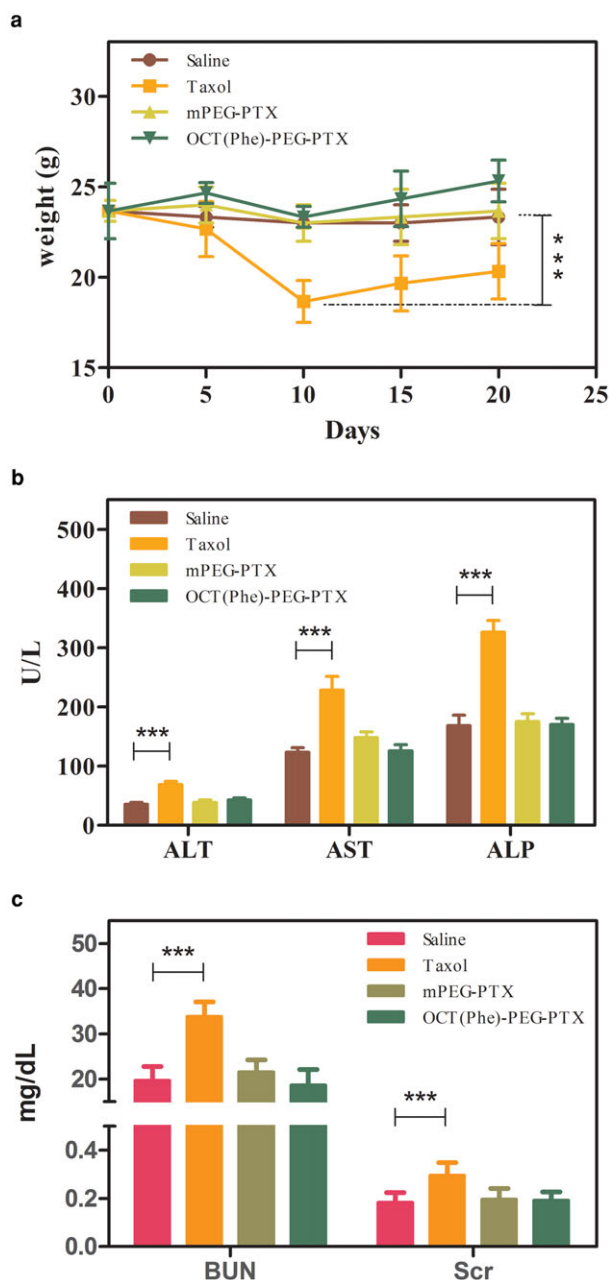


Figure 6. (a) Body weight changes in NCI-H446-bearing mice after intravenous injection of saline, Taxol, mPEG-PTX, and OCT(Phe)-PEG-PTX. (b) Liver and (c) kidney function test after treatment with saline, Taxol, PTX-loaded HA-DOCA micelles, and PTX-loaded HA-ss-DOCA micelles. Results are expressed as mean \pm SD ($n = 5$). * $p < 0.05$, ** $p < 0.01$ and *** $p < 0.001$ versus saline group.

REFERENCES

- de Weger VA, Beijnen JH, Schellens JH. 2014. Cellular and clinical pharmacology of the taxanes docetaxel and paclitaxel—A review. *Anticancer Drugs* 25(5):488–494.
- Andoh T, Kitamura R, Fushimi H, Komatsu K, Shibahara N, Kuraishi Y. 2014. Effects of goshajinkigan, hachimijiogan, and rokumigan on mechanical allodynia induced by paclitaxel in mice. *J Tradit Complement Med* 4(4):293–297.

- Lehoczký O, Bagameri A, Udvarý J, Pulay T. 2001. Side-effects of paclitaxel therapy in ovarian cancer patients. *Eur J Gynaecol Oncol* 22(1):81–84.
- Giang I, Boland EL, Poon GM. 2014. Prodrug applications for targeted cancer therapy. *AAPS J* 16(5):899–913.
- Qu D, Lin H, Zhang N, Xue J, Zhang C. 2013. In vitro evaluation on novel modified chitosan for targeted antitumor drug delivery. *Carbohydr Polym* 92(1):545–554.
- Ding Y, Chen W, Hu J, Du M, Yang D. 2014. Polymerizable disulfide paclitaxel prodrug for controlled drug delivery. *Mater Sci Eng C, Mater Biol Appl* 44:386–390.
- Jun YJ, Min JH, Ji da E, Yoo JH, Kim JH, Lee HJ, Jeong B, Sohn YS. 2008. A micellar prodrug of paclitaxel conjugated to cyclotriphosphazene. *Bioorg Med Chem Lett* 18(24):6410–6413.
- Kakinoki A, Kaneo Y, Tanaka T, Hosokawa Y. 2008. Synthesis and evaluation of water-soluble poly(vinyl alcohol)-paclitaxel conjugate as a macromolecular prodrug. *Biol Pharm Bull* 31(5):963–969.
- Zou Y, Fu H, Ghosh S, Farquhar D, Klostergaard J. 2004. Antitumor activity of hydrophilic paclitaxel copolymer prodrug using locoregional delivery in human orthotopic non-small cell lung cancer xenograft models. *Clin Cancer Res* 10(21):7382–7391.
- Makino A, Kimura S. 2014. Solid tumor-targeting theranostic polymer nanoparticle in nuclear medicinal fields. *Sci World J* 2014:424513.
- Duarte S, Faneca H, Lima MC. 2012. Folate-associated lipoplexes mediate efficient gene delivery and potent antitumoral activity in vitro and in vivo. *Int J Pharm* 423(2):365–377.
- Nkepan G, Bio M, Rajaputra P, Awuah SG, You Y. 2014. Folate receptor-mediated enhanced and specific delivery of far-red light-activatable prodrugs of combretastatin A-4 to FR-positive tumor. *Bioconjug Chem* 25(12):2175–2188.
- Aher N, Banerjee S, Bhansali S, Yadav R, Shidore M, Mhaske S, Chaudhari R, Asai S, Jalota-Badhwari A, Khandare J. 2013. Poly(ethylene glycol) versus dendrimer prodrug conjugates: Influence of prodrug architecture on cellular uptake and transferrin mediated targeting. *J Biomed Nanotechnol* 9(5):776–789.
- Zhou X, Wang H, Shi P, Meng AM. 2014. Characterization of a fusion protein of RGD4C and the beta-lactamase variant for antibody-directed enzyme prodrug therapy. *Onco Targets Ther* 7:535–541.
- Lee MH, Kim JY, Han JH, Bhuniya S, Sessler JL, Kang C, Kim JS. 2012. Direct fluorescence monitoring of the delivery and cellular uptake of a cancer-targeted RGD peptide-appended naphthalimide theragnostic prodrug. *J Am Chem Soc* 134(30):12668–12674.
- Tong GJ, Hsiao SC, Carrico ZM, Francis MB. 2009. Viral capsid DNA aptamer conjugates as multivalent cell-targeting vehicles. *J Am Chem Soc* 131(31):11174–11178.
- Mariniello B, Finco I, Sartorato P, Patalano A, Iacobone M, Guzzardo V, Fassina A, Mantero F. 2011. Somatostatin receptor expression in adrenocortical tumors and effect of a new somatostatin analog SOM230 on hormone secretion in vitro and in ex vivo adrenal cells. *J Endocrinol Invest* 34(6):e131–e138.
- Bison SM, Konijnenberg MW, Melis M, Pool SE, Bernsen MR, Teunissen JJ, Kwekkeboom DJ, de Jong M. 2014. Peptide receptor radionuclide therapy using radiolabeled somatostatin analogs: Focus on future developments. *Clin Transl Imaging* 2:55–66.
- Accardo A, Aloj L, Aurilio M, Morelli G, Tesaro D. 2014. Receptor binding peptides for target-selective delivery of nanoparticles encapsulated drugs. *Int J Nanomedicine* 9:1537–1557.
- Di Cianni A, Carotenuto A, Brancaccio D, Novellino E, Reubi JC, Beetschen K, Papini AM, Ginanneschi M. 2010. Novel octreotide dicarba-analogues with high affinity and different selectivity for somatostatin receptors. *J Med Chem* 53(16):6188–6197.
- Marsh HM, Martin JK Jr., Kvols LK, Gracey DR, Warner MA, Warner ME, Moertel CG. 1987. Carcinoid crisis during anesthesia: Successful treatment with a somatostatin analogue. *Anesthesiology* 66(1):89–91.
- Casar-Borota O, Heck A, Schulz S, Nesland JM, Ramm-Petersen J, Lekva T, Alafuzoff I, Bollerslev J. 2013. Expression of SSTR2a, but not of SSTRs 1, 3, or 5 in somatotroph adenomas assessed by monoclonal

antibodies was reduced by octreotide and correlated with the acute and long-term effects of octreotide. *J Clin Endocrinol Metab* 98(11):E1730–E1739.

23. Hodolic M, Fettich J, Rubello D. 2009. Influence of tumour size and uptake of ^{99m}Tc -octreotide on radio-guided surgery for neuroendocrine tumors. *Minerva Endocrinol* 34(2):89–96.

24. Spetz J, Dalmo J, Nilsson O, Wangberg B, Ahlman H, Forssell-Aronsson E. 2012. Specific binding and uptake of ^{131}I -MIBG and ^{111}In -octreotide in metastatic paraganglioma—Tools for choice of radionuclide therapy. *Hormone Metab Res* 44(5):400–404.

25. Iwase Y, Maitani Y. 2012. Dual functional octreotide-modified liposomal irinotecan leads to high therapeutic efficacy for medullary thyroid carcinoma xenografts. *Cancer Sci* 103(2):310–316.

26. Xu W, Burke JF, Pilla S, Chen H, Jaskula-Sztul R, Gong S. 2013. Octreotide-functionalized and resveratrol-loaded unimolecular micelles for targeted neuroendocrine cancer therapy. *Nanoscale* 5(20):9924–9933.

27. Vllasaliu D, Fowler R, Stolnik S. 2014. PEGylated nanomedicines: Recent progress and remaining concerns. *Expert Opin Drug Deliv* 11(1):139–154.

28. Kolate A, Baradia D, Patil S, Vhora I, Kore G, Misra A. 2014. PEG—A versatile conjugating ligand for drugs and drug delivery systems. *J Control Release* 192:67–81.

29. Vandana M, Sahoo SK. 2010. Long circulation and cytotoxicity of PEGylated gemcitabine and its potential for the treatment of pancreatic cancer. *Biomaterials* 31(35):9340–9356.

30. Maeda H. 2014. Research spotlight: Emergence of EPR effect theory and development of clinical applications for cancer therapy. *Ther Deliv* 5(6):627–630.

31. Cavallaro G, Licciardi M, Caliceti P, Salmaso S, Giammona G. 2004. Synthesis, physico-chemical and biological characterization of a paclitaxel macromolecular prodrug. *Eur J Pharm Biopharm* 58(1):151–159.

32. Li C, Yu DF, Newman RA, Cabral F, Stephens LC, Hunter N, Milas L, Wallace S. 1998. Complete regression of well-established tumors using a novel water-soluble poly(L-glutamic acid)-paclitaxel conjugate. *Cancer Res* 58(11):2404–2409.

33. Nie S, Hsiao WL, Pan W, Yang Z. 2011. Thermoreversible Pluronic F127-based hydrogel containing liposomes for the controlled delivery of paclitaxel: In vitro drug release, cell cytotoxicity, and uptake studies. *Int J Nanomedicine* 6:151–166.

34. Huo M, Zou A, Yao C, Zhang Y, Zhou J, Wang J, Zhu Q, Li J, Zhang Q. 2012. Somatostatin receptor-mediated tumor-targeting drug delivery using octreotide-PEG-deoxycholic acid conjugate-modified N-deoxycholic acid-O, N-hydroxyethylation chitosan micelles. *Biomaterials* 33(27):6393–6407.

35. Morisco A, Accardo A, Gianolio E, Tesaro D, Benedetti E, Morelli G. 2009. Micelles derivatized with octreotide as potential target-selective contrast agents in MRI. *J Peptide Sci* 15(3):242–250.

36. Xie W, Liu J, Qiu M, Yuan J, Xu A. 2010. Design, synthesis and biological activity of cell-penetrating peptide-modified octreotide analogs. *J Peptide Sci* 16(2):105–109.

37. Greenfield NJ. 2006. Using circular dichroism spectra to estimate protein secondary structure. *Nat Protoc* 1(6):2876–2890.

38. Cavallaro G, Maniscalco L, Campisi M, Schillaci D, Giammona G. 2007. Synthesis, characterization and in vitro cytotoxicity studies of a macromolecular conjugate of paclitaxel bearing oxytocin as targeting moiety. *Eur J Pharm Biopharm* 66(2):182–192.

39. Akinc A, Battaglia G. 2013. Exploiting endocytosis for nanomedicines. *Cold Spring Harbor Perspect Biol* 5(11):a016980.

40. Greish K. 2010. Enhanced permeability and retention (EPR) effect for anticancer nanomedicine drug targeting. *Methods Mol Biol* 624:25–37.